# Tunable Microwave Inductor Using Liquid-Metal Microfluidics

Alexander M. Watson\*#, Thomas F. Leary\*#, Jonathan Itokazu\$, Aji G. Mattamana\*, Tony Quach\*, Aaron T. Ohta\$, Wayne A. Shiroma\$, and Christopher E. Tabor\*

\*Air Force Research Laboratory, WPAFB, USA

#UES Inc, Dayton, OH, USA

\$University of Hawai'i at Mānoa, Honolulu, Hawaii, USA

Abstract— Room-temperature liquid metals such as eutectic gallium-indium (EGaIn) alloys have the potential to realize physically reconfigurable microwave components and circuits. Integrating microfluidic precision control of these liquid conductors with standard microwave board circuits enables a new paradigm of tunability for microwave components. One area that would greatly benefit from passive component agility is impedance-matching networks, where fine tuning the reactance is essential for reconfigurability. We demonstrate a microfluidic-integrated microwave inductor device that employs a high-impedance microstrip trace with three switchable taps to provide inductances of 1.2 nH, 1.9 nH and 2.3 nH at 5 GHz. Precise volumes of liquid metal are dispensed and confined to bridge existing gaps between copper microstrip traces to reconfigure the total length of the narrow trace, providing an effective method to tune the component's inductance.

Keywords— EGaIn, gallium alloy, liquid metal, microfluidic electronics, reconfigurable electronics, tunable inductors

## I. INTRODUCTION

Physically reconfigurable microwave components utilizing liquid-metal conductors have demonstrated highly tunable and adaptable performance beyond the traditional solutions of microelectromechanical systems (MEMS) or electrically tunable materials [1]. One crucial area where physically reconfigurable circuits can make an impact is in tuning matching networks, where small, precise changes on a circuit layout can greatly improve a device's performance within a network.

To date, many solutions from the field of MEMS and varactor materials have addressed the challenge from the capacitive side [2]. Yet effective impedance matching over a broader spectrum of frequencies can be significantly enhanced with a tunable inductor component [3]. The challenge of tunable inductance has been investigated from a material standpoint by employing magnetoelectric materials in conjunction with external magnetic fields [4], yet these solutions require bulky external magnets and preclude the independent tuning of multiple inductors in close proximity.

Microfluidics offers a platform of precision control of fluids on a chip that can be integrated with microwave circuits [5]. Gallium-indium alloys such as eutectic gallium

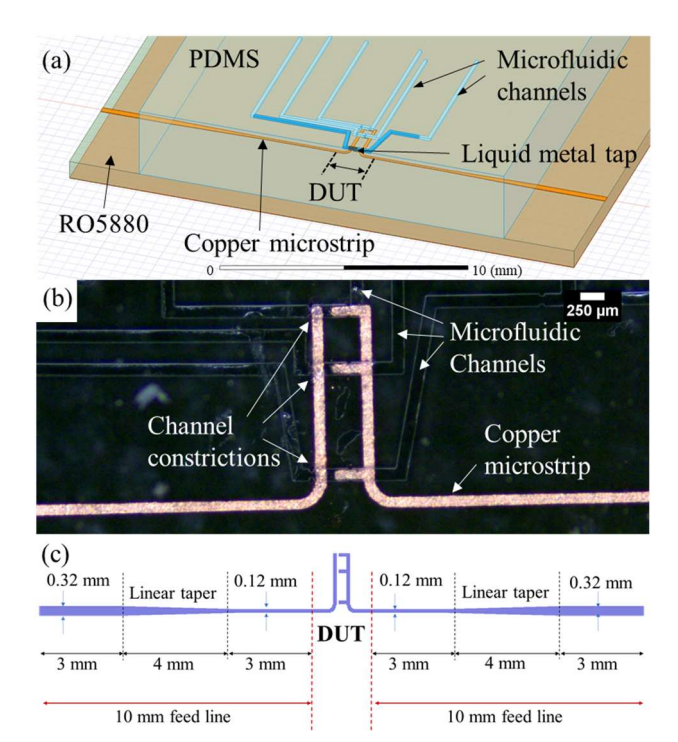


Fig. 1. (a) Cut out illustration of the integrated microfluidic and microstrip inductor device. (b) Top down image of the device as fabricated, including microfluidic channels with channel constrictions for liquid metal dosing. (c) Layout dimensions of the copper microstrip trace, depicting the DUT and the feed lines. The feeds taper wider to facilitate contact with the measurement probes.

indium (EGaIn) have been successfully employed as reconfigurable liquid conductors at room temperature [6], [7]. They provide high conductivity (3.40  $\times$  10 $^6$  S/m) and importantly are non-toxic, unlike mercury. Furthermore, by selecting appropriate co-fluids and using microfluidic designs techniques, liquid metals can be controllably reconfigured either pneumatically or electrostatically [8]. One such microfluidic technique is to design channels with various widths, which serve to confine the liquid metals by internal Laplace pressures; narrower constrictions require higher pneumatic or electrostatic pressure to create liquid

flow. These Laplace barriers have successfully been implemented as a method of precision control for liquid metals within microwave circuits [10]-[12].

Previously demonstrated liquid-metal tunable inductors use either mechanical stretching [13] or pneumatic pressure [14] to change inductance values and were not designed for microwave frequencies. In this paper, a switchable, high-impedance microstrip transmission line with three discrete gaps in the device are overlayed with microfluidic channels that are selectively filled with liquid metal to bridge the desired gap, demonstrating a simple method of inductance tuning in the microwave band. Each of these bridge points acts as a different tap for the high-impedance microstrip, altering the length of the device under test (DUT) to achieve a range of inductance.

#### II.DEVICE DESIGN

A microstrip transmission line was designed and fabricated with microfluidic channels bonded on the top of the board, as depicted in Fig. 1(a)-(b). The microchannels allow integration of the copper microstrip trace with liquid metal within the channels. The microstrip features a wider section on each end (to interface with the test fixture) that tapers down to a narrow, high-impedance trace. The narrow trace provides an increase in inductance with increasing trace length while minimizing parasitic capacitance to mitigate the effects of self-resonance [15]. The DUT consists of two traces running parallel to each other, while the tapered feed lines extend to the text fixture as illustrated in Fig. 1(c).

Each of the three taps along the length of the DUT has a separate microfluidic channel to allow individual control of the liquid metal that physically bridges the gap between the input and output copper traces, creating a switchable transmission line with three distinct lengths. A co-fluid of 1 M NaOH is used to remove the native oxide skin that forms on the liquid metal EGaIn, preventing pinning of the liquid metal within the channel. This co-fluid is used to demonstrate the proof-of-concept for switchable liquid-metal electronics; however, the operation does not require the NaOH, as other actuations methods from literature are compatible with this principle [16].

## A. Inductor Design and Fabrication

The target band of operation is from 1-10 GHz, covering L, S and C bands primarily used for microwave communication. A range of 0.5-5 nH for inductance was deemed appropriate when paired with typical ranges of tunable capacitors for this frequency range. Spiral and serpentine inductor designs were considered; however, the scale of the microfluidics integration is incompatible. Parasitic capacitance for these designs becomes prohibitively high, causing self-resonance within the frequency band of interest. Instead, the straightforward high-impedance microstrip

presents the best solution to achieve the desired inductance while accommodating the microchannels.

A high-impedance line was designed on a RO5880 board (Rogers Corp.) with 0.787-mm (31-mil) thickness, relative permittivity of  $\epsilon_r$  = 2.2, and ½ oz. copper metallization (17  $\mu m$  thick). The minimum trace width was 120  $\mu m$  to account for fabrication tolerances. All device samples and accompanying calibration samples were fabricated in the same batch with a roll-to-roll photolithography and etch process.

The overall length of the DUT must be on the order of millimeters to achieve inductances in the range of 0.5-5 nH. To facilitate the microfluidic layout and test measurement setup, the high-impedance microstrip is extended on either side of the DUT and tapered out to a wider trace to allow good contact with the test probe. These tapered feed line extensions are de-embedded from the measurement of the device as explained later.

#### B. Microfluidics Integration

Microfluidic channels fabricated in polydimethylsiloxane (PDMS) are bonded to the surface of the microstrip board to individually address each tap point between input and output trace at the DUT. The channels are routed away from the DUT to allow space for the fluid access ports. Constrictions in the channel width are used to generate discrete volumes of EGaIn and precisely position them to bridge the gaps in the copper traces. This technique is enabled by the high surface tension of EGaIn (624 mN/m in air, compared to 72 mN/m for water in air) [6], which requires an applied pressure in excess of the Laplace pressure formed by the EGaIn interface in the microchannel geometry to flow EGaIn into the channel constriction. The use of geometric constrictions in microfluidic channels as Laplace barriers to precisely control EGaIn has been previously demonstrated [10]-[12].

The microfluidic channels were fabricated using a standard soft lithography process. A mold was photopatterned in a 100-µm thick layer of SU-8 2035 (Microchem) epoxy photoresist on a silicon wafer using a transparency mask and MA6 mask aligner (Karl Suss). The PDMS (Sylgard 184) was mixed in the standard 10:1 ratio by weight of base and curing agent using a planetary mixer (Thinky). The mixture was cast onto the SU-8 mold, degassed, and cured at 65 °C for two hours. The cured PDMS was cut to size and fluidic access ports were cored to the 100-µm tall channels using a biopsy punch (1.5 mm, Integra Miltex).

A 20-μm film of PDMS was spin-coated at 4000 rpm (Spin-150, SPS-Europe) and cured at 100 °C for 35 minutes on the RO5880 board to enable the bonding of the channels. Before bonding, parts of the thin film PDMS that cover the copper were removed to allow the liquid-metal segments in the channels above to make electrical connection with the copper underneath. The 5-mm thick PDMS structure was

then aligned over the copper trace and bonded by exposing both surfaces to oxygen plasma (Harrick) for 30 seconds and pressing them into contact.

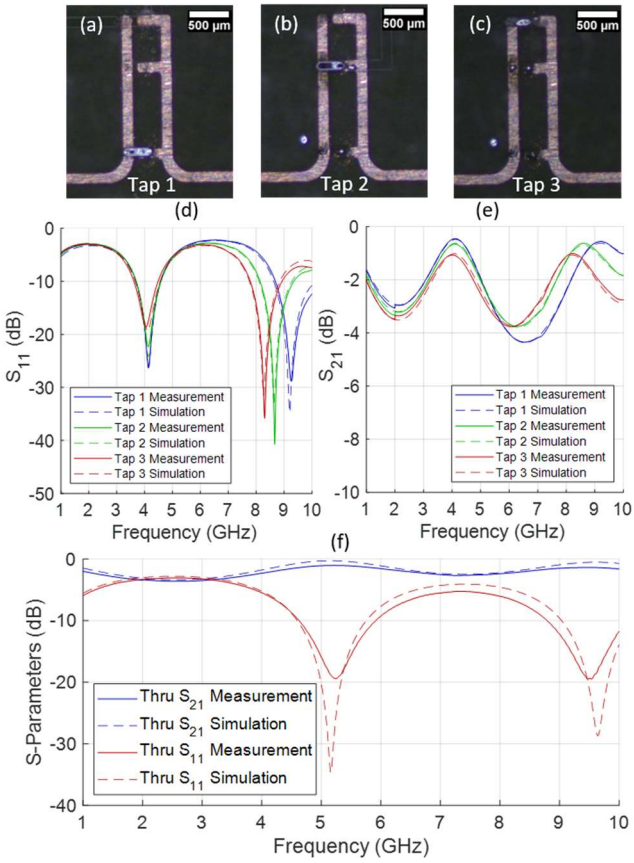


Fig. 2. (a)-(c) Images of the DUT connected by EGaIn segment at tap 1, tap 2, and tap 3 positions, respectively. (d)  $S_{II}$  and (e)  $S_{2I}$  measurements of the entire structure, including tapered feed lines for the three tap locations. (f) S-parameter measurements compared with simulations of the feed lines cascaded directly, without the DUT.

## III. DEVICE OPERATION AND PERFORMANCE

The electrical performance is measured by actuating the liquid metal over the desired tap and capturing S-parameter data, (Fig. 2). The device is measured using an Anritsu Universal Test Fixture that acts as an adapter between the board and the coaxial cables of the VNA (Keysight PNA 8362C). The measurement reference plane is calibrated to the edge of the test fixture where it meets the board, using a microstrip calibration kit (Anritsu 36804B-10M). The microchannels are dosed with liquid-metal segments using a microfluidic displacement system (Nordson Ultimus IV). Once liquid-metal loading is complete, the dispensing fluid is switched to the NaOH co-fluid. By increasing pressure on the co-fluid, the EGaIn segment is pushed beyond the channel constriction to electrically bridge the gap in the

copper traces. Once connected, S-parameter data is captured. Images of the three taps connected individually are depicted in Fig. 2(a)-(c).

Models of the entire structure are created within ANSYS HFSS to corroborate the measurement, and show good agreement with measurements, [Fig. 2(d)-(e)]. However, an accurate measurement de-embedding process to remove the effects of the tapered feed lines is not possible, due to the PDMS superstrate spanning across the reference plane between feed line and DUT, preventing the test fixture probe at this point, and therefore disallowing a full 2-port measurement of either feed line alone.

When in-fixture measurements for de-embedding aren't possible, extraction of the DUT from measurements typically involves a TRL calibration. Thru, reflect, and line calibration standards were fabricated alongside the device samples, however the implementation of the TRL calibration yielded unreliable results. This is likely due to the distance between the launch and the DUT, as confined by the physical length restrictions of the microstrip test fixture. It's recommended to allow two-wavelength separation between the launch and the DUT to prevent higher order modes from producing undesired variations in error-corrected measurement [17]. Since this separation is not possible with the test fixture at 10 GHz, we extracted the DUT as follows.

First, to further validate the HFSS model, the Thru TRL calibration standard, consisting of the two tapered feed lines cascaded directly, is measured and compared with models of the same, [Fig. 2(f)]. Since the HFSS models of the entire structure (DUT and feed lines) and the feed lines cascaded directly (TRL Thru) corroborates the measurements, the HFSS model of the DUT alone is used to determine the inductance of the DUT itself.

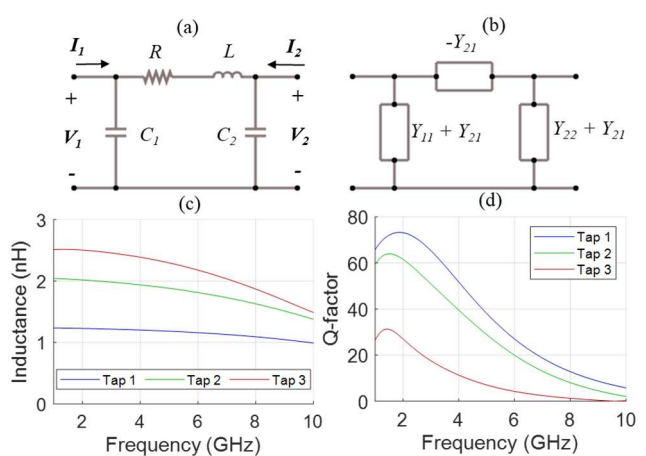


Fig. 3. (a) Lumped circuit model and (b) Y-parameter network representation of the high-impedance microstrip line. Inductance is extracted from the imaginary part of the  $Y_{2l}$  parameter of a 2-port measurement. (c) Extracted inductance of the DUT for the three discrete taps using the HFSS model that is corroborated by measurements of both the entire structure and only feed lines. (d) Modeled Q-factor of the DUT inductor device for the three taps.

As depicted in Fig. 3(a), the transmission line is modelled with a nominal pi model which can be understood as a network of admittances, with admittances  $Y_1$  and  $Y_2$  corresponding to the shunt capacitances respectively, and  $Y_3$  corresponding to the combined series resistance and inductance of the line. Calculating Y-parameters from this pi model is straightforward, as  $Y_{11}$  is defined as  $I_1/V_1$  while port 2 is shorted, giving  $Y_{21} = Y_1 + Y_3$ . The  $Y_{21}$  parameter is defined as  $I_2/V_1$  while port 2 is shorted, giving  $Y_{21} = -Y_3$ . By symmetry,  $Y_{22} = Y_2 + Y_3$  and  $Y_{12} = Y_{21}$ . Finally, these expressions of admittance can be solved in terms of the Y-parameters to arrive at the pi model shown in Fig. 3(b). Using these Y-parameters allows for extraction of the inductance in the series portion of the pi network, governed by

$$L = \frac{Im\left\{-\frac{1}{Y_{21}}\right\}}{2\pi f}.$$
 (1)

Extracted values of the inductance for the three taps are shown in Fig. 3(c). At 5 GHz, the inductance values are 1.2 nH, 1.9 nH, and 2.3 nH for Taps 1, 2, and 3, respectively. The self-resonance frequency for the inductive microstrip exceeds 10 GHz as designed, to allow for the full inductance tuning range over the desired band from 1-10 GHz. The extracted *Q*-factor is shown in Fig. 3(d), with values of 38.2, 28.9 and 7.1 at 5 GHz for Taps 1, 2 and 3, respectively.

#### IV. CONCLUSION

We have demonstrated a physically reconfigurable series inductance device capable of switching its inductance between 1.2 nH, 1.9 nH and 2.3 nH at 5 GHz. The device shows a broadband reconfigurable inductance from 1-10 GHz. While a simple three-tap device is shown here, the method of microfluidics integration of liquid metal and microstrip traces can be scaled to various inductance ranges and resolutions, depending on the design space requirements.

# ACKNOWLEDGMENT

This work was supported in part by the U.S. National Science Foundation under Grant ECCS-1807896.

# REFERENCES

- [1] K. Entesari and A. P. Saghati, "Fluidics in microwave components," in *IEEE Microwave Magazine*, vol. 17, no. 6, pp. 50-75, June 2016.
- [2] G. M. Rebeiz, K. Entesari, I.C. Reines, S. Park, M.A. Eltanani, A. Grichener, and A.R. Brown., "Tuning in to RF MEMS," in *IEEE Microwave Magazine*, vol. 10, no. 6, pp. 55-72, Oct. 2009.
- [3] A. Saberkari, S. Ziabakhsh, H. Martinez, and E. Alarcón, "Active inductor-based tunable impedance matching network for RF power amplifier application," *Integration*, vol. 52, pp. 301-308, Jan. 2016.

- [4] J. Lou, M. Liu, and N.X. Sun, "Electrostatically tunable magnetoelectric inductors with large inductance tenability," *Appl. Phys. Lett.*, vol. 94, pp. 112508, Mar. 2009.
- [5] S. Cheng and Z. Wu, "Microfluidic electronics," *Lab Chip*, vol. 12, pp. 2782-2791, 2012.
- [6] M. D. Dickey, "Stretchable and soft electronics using liquid metals," *Adv. Mater.*, p. 1606425, 2017.
- [7] G. Zhang, R. C. Gough, M. M. Moorefield, A. T. Ohta, and W. A. Shiroma, "An electrically actuated liquid-metal switch with metastable switching states," in 2016 IEEE MTT-S IMS, May 2016.
- [8] R. C. Gough, A. M. Morishita, J. H. Dang, M. R. Moorefield, W. A. Shiroma, and A. T. Ohta, "Rapid electrocapillary deformation of liquid metal with reversible shape retention," *Micro and Nano Systems Lett.*, vol. 3, no. 4, 2015.
- [9] A. V. Diebold, A. M. Watson, S. Holcomb, C. E. Tabor, D. Mast, M. D. Dickey, and J. Heikenfeld, "Electrowetting-actuated liquid metal for RF applications," *J. Micromech. Microeng.*, vol. 27, no. 2, p. 025010, 2017.
- [10] E. Kreit, M. Dhindsa, S. Yang, M. Hagedon, K. Zhou, I. Papautsky, and J. Heikenfeld, "Laplace barriers for electrowetting thresholding and virtual fluid confinement," *Langmuir*, vol. 26, no. 23, pp. 18550-18556, 2010.
- [11] M. R. Khan, G. J. Hayes, J.-H. So1, G. Lazzi, and M. D. Dickey, "A frequency shifting liquid metal antenna with pressure responsiveness," *Appl. Phys. Lett.*, vol. 99, pp. 013501, Jun. 2011.
- [12] A.M. Watson, T. F. Leary, K. S. Elassy, A. G. Mattamana, M. A. Rahman, W. A. Shiroma, A. T. Ohta, and C. E. Tabor, "Physically reconfigurable RF liquid electronics via Laplace barriers," *IEEE Trans. Microw. Theory and Tech.*, vol. 67, 4881-4889, Dec. 2019.
- [13] N. Lazarus, C. D. Meyer, S. S. Bedair, H. Nochetto, and I. M. Kierzewski, "Multilayer liquid metal stretchable inductors," *Smart Materials and Structures*, vol. 23, p. 085036, 2014.
- [14] N. Lazarus and S. S. Bedair, "Bubble inductors: pneumatic tuning of a stretchable inductor," *AIP Advances*, vol. 8, p. 056601, 2018.
- [15] "Application Note AN 258," Infinion Technologies, Munich, Germany.
- [16] I. D. Joshipura, H. R. Ayers, G. A. Castillo, C. Ladd, C. E. Tabor, J. J. Adams, and M.D. Dickey, "Patterning and reversible actuation of liquid gallium alloys by preventing adhesion on rough surfaces," ACS Appl. Mater. Inter., vol. 10, 44686-44695, 2018.
- [17] Agilent Technologies, "Network analysis applying the 8510 TRL calibration for non-coaxial measurements," Product Note 8510-8A, 2000.